International Journal of Research
Available at https://edupediapublications.org/journals
p-ISSN: 2348-6848
e-ISSN: 2348-795X
Volume 03 Issue 11
July 2016

Hybrid RES with Fuzzy based Predictive Control for Shipboard Using the IPA-SQP

AMBALA SUJITH KUMAR
M-tech Student Scholar
Department of Electrical & Electronics Engineering,
Malla Reddy Engineering College, Maisammaguda, Dhulapally RD; Kompally; Hyderabad
RR Dist. (Dt); Telangana, India.

MRS. K ANITHA REDDY
Assistant Professor
Department of Electrical & Electronics Engineering,
Malla Reddy Engineering College, Maisammaguda, Dhulapally RD; Kompally; Hyderabad
RR Dist. (Dt); Telangana, India.

Abstract – Shipboard power distribution systems and their first cousins in the terrestrial world have common fundamental characteristics. They use a variety of interconnected components to transport electrical energy, safely and reliably, from a source of supply to end users and loads. Shipboard integrated power systems, the key enablers of ship electrification, call for effective power management control (PMC) to achieve optimal and reliable operation in dynamic environments under hardware limitations and operational constraints. The design of PMC can be treated naturally in a model predictive control (MPC) framework, where a cost function is minimized over a prediction horizon subject to constraints. The power generation in ship system will include in high cost and complex. In order to reduce these problems renewable energy sources can be used with the power management with photo voltaic cell and fuel cell applications. Several operational scenarios are considered to evaluate the performance of the proposed PMC solution. Different performance attributes and their tradeoffs can be coordinated through proper tuning of the design parameters. In this paper a fuzzy based Model predictive control (MPC) is an effective control methodology that exploits the solution of a receding horizon optimal control problem to enforce constraints, such as the operational limits of the IPS, and to shape its high transient response is evaluated with Matlab/simulink analysis.

Index Terms— Integrated perturbation analysis and sequential quadratic programming (IPA-SQP), integrated power system (IPS), model predictive control (MPC), power management control (PMC), real-time optimization.

I. INTRODUCTION

Shipboard integrated power systems (IPSs) have been pursued as the key enabling technology in ship electrification for applications including warships and high-value commercial ships [1], [2]. They provide electrical power for both the propulsion system and service loads, and rely on power management control (PMC) strategies to coordinate the power sources and loads to achieve efficient and robust operation and to meet various dynamic requirements in diverse and sometimes adverse conditions. Moreover, effective PMC strategies are expected to provide improved fuel efficiency, enhanced response speed, and superior reliability [3]. To accomplish this, PMC must effectively deal with nonlinear system dynamics and stringent constraints that protect system components. In addition, PMC must be simple to tune to be able to trade off and rebalance performance attributes.

Several approaches have been proposed for shipboard PMC with IPS. An automatic rule-based expert system is proposed for reconfiguration of shipboard IPS to enhance survivability of naval ships in [4]. In [5], an automated self-healing strategy is investigated by solving an optimization problem with constraints using a linear programming algorithm. In [6], a decentralized control approach using an intelligent multi agent system for shipboard power systems is proposed. Several research groups have developed shipboard PMC strategies using the real-time optimization framework.

p-ISSN: 2348-6848
e-ISSN: 2348-795X
Volume 03 Issue 11
July 2016

For example, a fast reconfiguration algorithm based on zone selection differential protection schemes is reported in [7]; however, [7] provides no evidence that the algorithm can be implemented in real time. In other studies, real-time simulations are achieved. For example, in [8], using the small population-based particle swarm optimization method, a fast intelligent reconfiguration algorithm is implemented on a real-time simulator. Seenumani *et al.* [9] pursue a methodology that exploits time-scale separation to achieve real-time optimization of a shipboard IPS. By solving a two-level simplified optimization problem, the computational efficiency is improved and these improvements are validated on a real-time simulator. In fact, studies of optimization based PMC strategies typically demonstrate implementation feasibility using only real-time simulations. To the best of our knowledge, however, no study has demonstrated the feasibility of optimization-based PMC with test results on a physical platform. In this paper, we design a PMC for a shipboard power system that includes multiple power sources and loads such as the ship propulsion system (SPS) and high-power electrical load (a pulsed-type load that represents an electromagnetic rail guns and/or an electromagnetic launch system). We consider the high-power electrical load as an unknown disturbance to the shipboard power system. The PMC is developed in a real-time optimization framework where a cost function is formulated and minimized while constraints that reflect design objectives and operational limitations are enforced.

The PMC design, which aims to meet load demands, save fuel, extend generator life cycle, and assure the power quality of the shipboard microgrid, is formulated as a nonlinear model predictive control (NMPC) problem with constraints. Model predictive control (MPC) is an effective control methodology that exploits the solution of a receding horizon optimal control problem to enforce constraints, such as the operational limits of the IPS, and to shape its transient response [10]–[12]. The ability to solve this optimal control problem in real time, i.e., within one sampling period, is, however, a key requirement for shipboard power management systems. This real-time requirement is very challenging as the system dynamics are fast and the sampling period in these applications is in the order of milliseconds. As in [13] and [14], the time and effort required for on-board NMPC computations need to be reduced as much as possible.

The inability to complete the computations of NMPC law in real time can result in loss of stability and degraded performance. Without assured real-time capability, it is also impossible to certify and use such a controller in safety critical applications such as the shipboard power management. Efficient numerical algorithms have been proposed to address challenges in the real-time implementation of MPC. Diehl *et al.* [15] and Cannon [16] provide an overview of efficient numerical methods and algorithms that have been developed for NMPC. Several algorithms, such as the nonlinear real-time iteration scheme [17]–[20], the Newton-type solver [21], and the continuation and generalized minimum residual [22], have a common feature that they perform one iteration of root finding in each sampling period.

The accuracy of finding the solution may, however, be insufficient, and the performance may be degraded for systems with significant nonlinearities. The advanced step algorithm [23] performs a complete Newton-type interior point procedure to convergence to avoid the potential issues associated with the early termination approaches. In [24], the feasibility-perturbed sequential quadratic programming (FP-SQP) algorithm has been proposed. To reduce the computation time, the FP-SQP algorithm maintains all intermediate iterations feasible and exploits suboptimal solutions. In this paper, we explore the integrated perturbation analysis and SQP (IPA-SQP) framework to develop a PMC. The IPA-SQP approach, developed for NMPC in [25]–[27], combines solution updates derived using perturbation analysis (PA) and SQP. For PA-based update, IPA-SQP exploits neighbouring external (NE) optimal control theory extended to discrete-time systems with constraints [28] to improve computational efficiency. The solution at time t is obtained as a correction to the solution at time $(t-1)$ through the NE update. If the NE update is not fulfilling optimality criteria, one or multiple SQP updates are exploited until the optimality criteria are satisfied.

The merged PA and SQP updates yield a fast solver for NMPC problems [29]. The IPA-SQP algorithm is based on the optimal control and NE theory, which results in efficient updates that are based on backward-in-time solution to discrete-time Riccati equations. Alternative methods based on the sensitivity of the underlying nonlinear programming problem [30]–[32] can also be exploited. The comparison between various approaches is beyond the scope of this paper and is left to future work. In this paper, we report the results of applying the IPA-SQP algorithm to solve the real-time MPC problem for shipboard PMC. Toward this end, a simplified optimization-oriented design model is derived by approximating components of the transient power management model (TPMM) [33], which is a low-order simulation model of the test bed at Purdue University. We then develop the IPA-SQP-based MPC controller and analyze the performance using the TPMM as the virtual test bed through both non real-time and real-time simulations. Finally, the algorithm is implemented on the physical test bed to evaluate its performance in several proposed operational scenarios. The capability to perform the computations in real time, satisfy constraints, and tune the performance attributes is demonstrated.

This paper is organized as follows. In Section II, the shipboard power system and its control objectives are described, and the simulation model is introduced. The optimization-oriented design model of the TPMM is derived by approximation and model order reduction. Then, the MPC problem with constraints is formulated considering various PMC operational requirements and constraints. In Section III, the features of the IPA-SQP-based MPC are reviewed and the algorithm of the IPA-SQP is described. Test scenarios of the proposed PMC for simulations and experiments are discussed in Section IV. The simulation results with the TPMM serving as the virtual test bed on a real-time simulator are reported and analyzed. The experimental results on the physical test bed are presented, analyzed, and compared with the simulation results. Section V ends this paper with the conclusion.

II. SYSTEM DESCRIPTION AND MPC FORMULATION

A. System Description The notional power system considered in this paper represents a scaled-down version of a real shipboard power system. It consists of two power generation systems, a ship propulsion motor, and a square-wave pulse power load (SWPPL). This system was developed at Purdue University as an outcome of a sponsored project by the Office of Naval Research [33], and has been used for several sponsored research projects [33], [34]. The schematic of the system is shown in Fig. 1, and the physical appearance of the test bed is shown in Fig. 2. Generation system 1 (GS-1) is the main shipboard power source and represents a gas turbine generator. Generation system 2 (GS-2) represents a smaller ship power generation source, such as a diesel generator. The SPS is the primary load on the power system. The SWPPL represents the load of an electromagnetic rail gun. The power sources and loads are

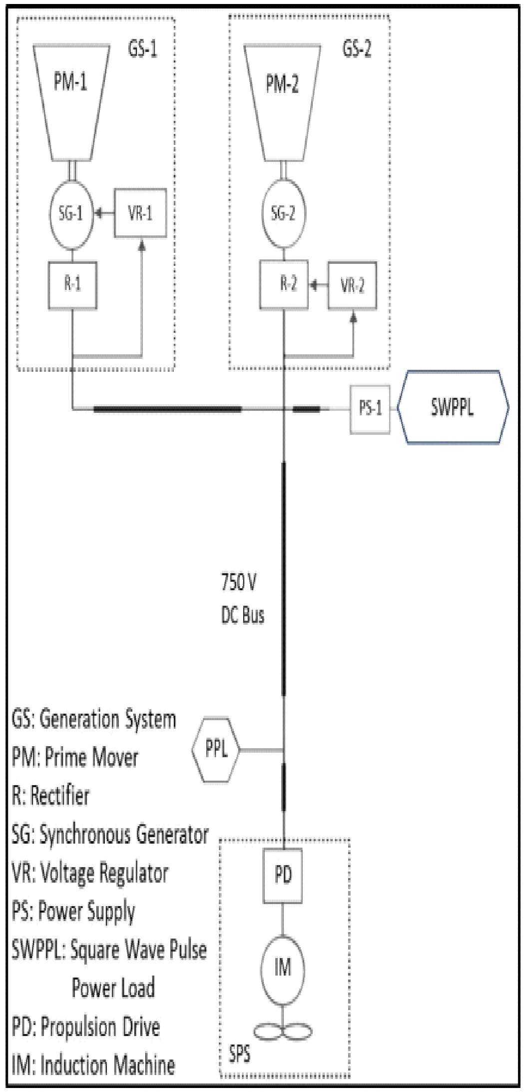

Fig. 1. Schematic of the shipboard power system.

International Journal of Research
Available at https://edupediapublications.org/journals
p-ISSN: 2348-6848
e-ISSN: 2348-795X
Volume 03 Issue 11
July 2016

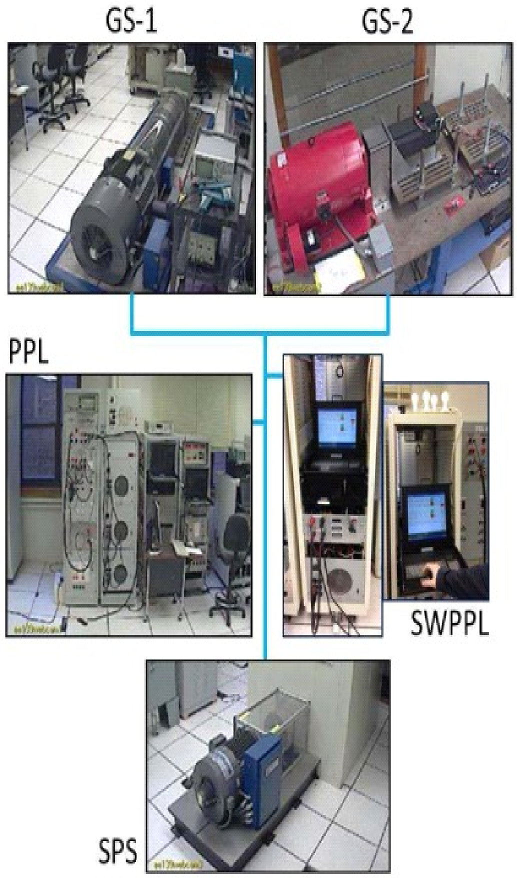

Fig. 2. Physical test bed.

connected in parallel to a 750 V dc bus. The key components and their operational parameters are listed in Table1.

B. Operational Requirements and Control Objectives For the investigation reported in this paper, we make the following assumptions that are representative of the physical system in the test bed. 1) The desired ship velocity, the SPS induction machine (IM) power and desired speed, and the target bus voltage are constant. 2) The GS-2 operates in the generation mode, has its best efficiency at 5 kW, and has a constant rotor speed.

TABLE I
SUBSYSTEMS OF THE TEST BED

Subsystems	Description	Key operational parameters
GS-1	Prime mover 1 Wound rotor synchronous machine	1800 rpm max. 59 kW
GS-2	Prime mover 2 Permanent magnet synchronous machine	3600 rpm max. 11 kW
SPS	Propulsion drive Induction machine	1800 rpm max. 37 kW
SWPPL	High power buck converter	peak 8 kW average 4 kW

International Journal of Research
Available at https://edupediapublications.org/journals
p-ISSN: 2348-6848
e-ISSN: 2348-795X
Volume 03 Issue 11
July 2016

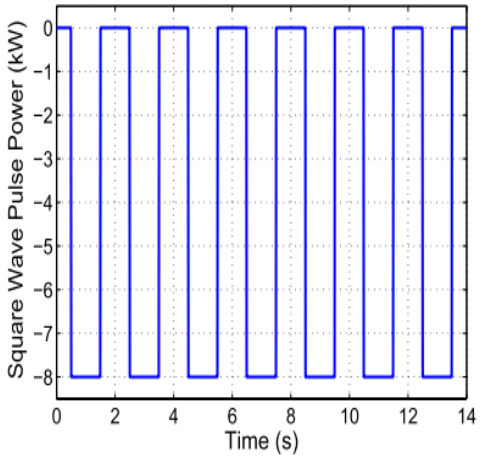

Fig. 3. SWPPL on the TPMM. The pulse starts at 0.5 s with 8-kW amplitude and 1-s duration. The period is 2 s.

3) The pulsed power load consists of square-wave pulses with 8-kW amplitude and 1-s duration (Fig. 3).
4) The PMC has no prior knowledge of the SWPPL, i.e., the SWPPL is an unknown disturbance.
5) The line losses are negligible.
Note that the above-listed assumptions are made to simplify the exposition of the algorithm or to reflect the hardware limitations (such as assumption 3). They can be removed or modified without changing the nature of the problem and the proposed solution.

The control objectives of the PMC are to coordinate the power generation sources to meet the load demand and to achieve the following performance attributes:
1) tracking the set points of bus voltage, GS-2 electrical power, SPS electrical power, and SPS rotor speed;
2) protecting and extending the life span of the machines GS-1, GS-2, and SPS;
3) Maintaining power quality of the microgrid and minimizing bus voltage variation.

We note that the GS-1 is expected to provide most of the power for SWPPL, which may cause extreme ramping in GS-1 power output due to the set-point tracking objective on GS-2 electrical power and, consequently, have negative impact on the gas turbine and generator life span. Therefore, some of the control objectives are competing with each other and need to be balanced by the PMC system.
C. Optimization-Oriented Design Model and Operational Constraints The TPMM is a low-order simulation model of the physical test bed that has been established by Purdue University.

TABLE II
STATE VARIABLES, CONTROL INPUTS, AND PARAMETERS IN THE OPTIMIZATION-ORIENTED DESIGN MODE

International Journal of Research
Available at https://edupediapublications.org/journals
p-ISSN: 2348-6848
e-ISSN: 2348-795X
Volume 03 Issue 11
July 2016

Variable	Symbol	Description
State variables	x_1	GS-1 electrical power (kW)
	x_2	IM rotor speed in the SPS (rad/s)
	x_3	DC bus voltage (V)
Control inputs	u_1	GS-1 droop gain
	u_2	GS-2 mechanical power command (kW)
	u_3	SPS mechanical power command (kW)
Parameters	T_s	Sampling time interval (s)
	ω_d	Desired rotor speed of the IM (rpm)
	V_b	Desired bus voltage (V)

It represents the essential dynamics of the power system developed in [33]. Even though the TPMM is already simplified to enable fast simulation, it is still complex to be used for the IPA-SQP algorithm implementation.

The optimization-oriented design model that supports analytical derivations for the IPA-SQP algorithm implementation is developed by simplifying the TPMM model. This model is represented by the following nonlinear discrete-time equations:

$$x_1(k+1) = f_1(x(k), u(k)) = x_1(k) + \frac{T_s x_3(k+1)}{x_3(k+1) + c_1 u_1(k)} z(k) \quad (1)$$

$$x_2(k+1) = f_2(x(k), u(k)) = \frac{1}{1 + T_s c_2 c_3}\left(x_2(k) + T_s c_2 (c_3 \omega_d + c_4 u_3(k))\right) \quad (2)$$

$$x_3(k+1) = f_3(x(k), u(k)) = \frac{1}{1 + T_s c_5}\left(x_3(k) + T_s \sqrt{c_6 x_3^2(k) + c_7 P_s(k)}\right) \quad (3)$$

Equations (1)–(3) are derived from the TPMM model based on several simplifying assumptions and approximations [33] and discretized using the backward Euler method. Table II summarizes the state variables, the control inputs, and parameters in (1) (3). The droop gain $u1$ of the voltage controller in the GS-1 is a control input. This GS-1 droop gain impacts the dc bus voltage. It is used to indirectly control the output power of the GS-1. The GS-2 and SPS receive the GS-2 and SPS mechanical power commands from the PMC, respectively. Then, their inner loop controllers convert the power commands to torque commands and current commands to accomplish tracking of these power commands using hysteresis control [33]. $P2(k)$ and $P3(k)$ are the GS-2 and SPS electrical power, respectively, and $P4(k)$ is the square-wave pulse power at sampling instant k. $Ps(k)$ is the sum of the GS-1, GS-2, SPS electrical power, and the SWPPL power at sampling instant k. These values are required to estimate GS-2 electrical power, SPS electrical power, the SWPPL power, and the sum of the electrical power with the state variables and control inputs at sampling instant k. The parameters ci, $i = 1,\ldots, 12$, are constants used in the equations [33]. Positive sign is used for electrical power generated, and negative sign is used for electrical power consumed. The system has several constraints that represent hardware limitations and operational requirements. The GS-1, GS-2, and SPS have operational limitations of 59, 11, and 37 kW, respectively, as given in Table I. The GS-1 droop gain takes values in the interval [−1, 1]. The constraints are mathematically expressed as

$$0 \le x_1(k) \le 59 \tag{4}$$

$$-1 \le u_1(k) \le 1 \tag{5}$$

$$-11 \le u_2(k) \le 0 \tag{6}$$

$$0 \le u_3(k) \le 37. \tag{7}$$

Note that the system is nonlinear with constraints that include a pure state constraint (4) and pure control constraints (5)–(7). Since the model is nonlinear, the NMPC approach is pursued to provide re-configurability to changing model parameters, requirements, and faults.

D. MPC Problem Formulation The MPC problem is formulated by considering the control objectives and operational assumptions

$$\min_{\substack{x(\cdot)\in\mathbb{R}^3,\\ u(\cdot)\in\mathbb{R}^3}} J(x(\cdot), u(\cdot)) \tag{8}$$

$$J(x(\cdot), u(\cdot)) = \Phi(x(t+N)) + \sum_{k=t}^{t+N-1} L(x(k), u(k)) \tag{9}$$

for all $k \in [t, t + N - 1]$, subject to (1)–(3) and (4)–(7). Here, $P2d$ and $P3d$ are the desired GS-2 electrical power and the desired SPS electrical power, respectively. xt is the state at a sampling instant t. $k j, j = 1,..., 8$, denote weighting factors on different terms in the cost function.

TABLE III
WEIGHTING FACTORS IN THE COST FUNCTION ON THE TEST BED

Physical meaning on the test bed	Weight	Test A (Baseline)	Test B (Increase k_6)	Test C (Increase k_3)
DC bus voltage deviation	k_1	1	1	1
GS-2 power deviation	k_2	15	15	15
SPS power deviation	k_3	15	15	**25**
SPS induction machine speed deviation	k_4	1	1	1
Ramp rate of GS-1 droop gain	k_5	13	13	13
Ramp rate of GS-1 power	k_6	1	**10**	**10**
Ramp rate of GS-2 power	k_7	0.1	0.1	0.1
Ramp rate of SPS power	k_8	0.1	0.1	0.1
SPS induction machine speed deviation	ϕ_1	100	100	100
DC bus voltage deviation	ϕ_2	100	100	100

Each weighting factor $k j$ assigns a relative priority to a performance aspect. The first term in $L(x(k), u(k))$, the error between the measured bus voltage and the desired bus voltage, is related to bus voltage tracking. Minimizing this error helps assure power quality on the microgrid.

The second term is for GS-2 to operate at the most efficient point. The other terms reflect SPS electrical power tracking of the desired value, SPS rotor speed tracking for maintaining the desired ship velocity, droop gain ramp rate, GS-1 electrical power ramp rate, GS-2 electrical power ramp rate, and SPS electrical power ramp rate. Component wear is reduced by penalizing power ramp rate. The $(x(t + N))$ is the terminal cost function to penalize the deviation of $x2(t + N)$ and $x3(t + N)$ from their desired values with weighting factors of $\varphi 1$ and $\varphi 2$, respectively. The GS-1 is treated as a slack generator and provides the power necessary to balance the generating power and consumed power. Hence, $x1(k)$ is not penalized. The values of the weighting factors used for the cost function are listed in Table III. Solving the MPC problem (8) subject to the constraints in real time requires an effective optimization algorithm. The IPA-SQP algorithm, which has been shown to have advantages in computational efficiency for NMPC [29], is reviewed in Section III.

III. OVERVIEW OF IPA-SQP ALGORITHM

p-ISSN: 2348-6848
e-ISSN: 2348-795X
Volume 03 Issue 11
July 2016

The IPA-SQP algorithm combines the complementary features of PA and SQP for solving constrained dynamic optimization problems [26], [27], [35], [37]. PA is an approach to predict a change in the optimal solution when some of the parameters, such as the initial conditions, are changed. The PA provides closed-form solutions and makes the optimization computationally efficient. Because of the approximate nature of the PA solution, however, it does not guarantee successive optimality when the algorithm is applied repeatedly to update a nominal solution. To correct the solution so that it satisfies the necessary conditions to a specified tolerance, an SQP update based on linearization and quadratic cost approximation can be applied. Through synergetic integration of these two algorithms, the optimal control sequence at each sampling instant t with the observed state $x(t)$ is calculated using the optimal control sequence from the previous sampling instant $(t-1)$. It can be shown that the IPA-SQP has a linear computational complexity of $O(N)$ as compared with SQP that has complexity from $O(N1.5)$ to $O(N3)$, where N is the prediction horizon of the MPC problem [29]. Moreover, the IPA-SQP has the following features. 1)The IPA-SQP efficiently computes the approximation of the optimal solution by taking advantage of backward-in time recursive updates. 2) When active constraints are not changed by the perturbation, $\delta x(t) = x(t) - x(t-1)$, in the initial state, the closed-form PA solution can be derived, thereby leading to a very efficient computation. If the variation $\delta x(t)$ in the initial state causes changes in the activity status of constraints, the variation $\delta x(t)$ is divided into smaller segments so that the PA solution can be applied to each of these segments to sequentially update the solution. It has been shown in several applications that a good tradeoff between efficient computation and accurate optimization can be achieved [25], [27], [37]. Let C and $\bar{C}$ denote the mixed state-input constraints and pure state constraints

$$C = \begin{pmatrix} -u_1 - 1 \\ u_1 - 1 \\ -u_2 - 11 \\ u_2 \\ -u_3 \\ u_3 - 37 \end{pmatrix}, \quad \bar{C} = \begin{pmatrix} -x_1 \\ x_1 - 59 \end{pmatrix}. \qquad (10)$$

The IPA-SQP algorithm computes the new control sequence over the prediction horizon in the form of

$$u^{(i+1)}(k) = u^{(i)}(k) + \delta u^{(i)}(k) \qquad (11)$$

$$\delta u^{(i)}(k) = -\begin{pmatrix} I & 0 \end{pmatrix} K_0(k) \times \begin{pmatrix} Z_{21}(k)\delta x^{(i)}(k) + f_u(k)^T T(k+1) + H_u(k) \\ \tilde{C}_x^a(k)\delta x^{(i)}(k) \end{pmatrix} \qquad (12)$$

And i is the iteration index. For $i = 0$, $u(0)(k)$ is taken as the solution sequence calculated at the previous sampling instant $(t-1)$. The matrices $K0$, $Z21$, $C \tilde{}\ x\ a$, and T are defined by the IPA-SQP algorithm. The detailed calculation steps are given in the Appendix. Hu and fu are the partial derivatives of the Hamiltonian function (13) and of the right-hand side of (1)–(3), i.e., $f(k) = (f1(k)\ f2(k)\ f3(k))T$ with respect to u, evaluated at $u(i)(k)$, respectively. Note that the predictor update is integrated with a corrector update that accounts for nonzero Hu. In the IPA-SQP algorithm, we terminate the iterations if $t\ k+ =N\ t -1$ $|Hu(k)| < Hu\ t$ for some small threshold $H\ tu$. A good tradeoff can be achieved between efficient computation and accuracy of the optimization by properly selecting $Hu\ t$, for instance, [38] where the tradeoff between computation time and optimality is illustrated for a spacecraft relative motion control problem in which the impact of different termination thresholds is evaluated. In this paper, $Hu\ t$ was chosen as 0.01 both in the simulations and experiments. Several iterations may be needed to satisfy the criterion $t\ k+ =N\ t -1$ $|Hu(k)| < Hu\ t$. The algorithm realization is based on a combination of a MATLAB script function and some Simulink blocks from the standard Simulink library. Fig. 4 shows the key steps of the IPA-SQP algorithm in the form of a pseudo code.

- IV INTRODUCTION TO FUZZY LOGIC CONTROLLER

L. A. Zadeh presented the first paper on fuzzy set theory in 1965. Since then, a new language was developed to describe the fuzzy properties of reality, which are very difficult and sometime even impossible to be described using conventional methods. Fuzzy set theory has been widely used in the control area with some application to dc-to-dc converter system. A simple fuzzy logic control is built up by a group of rules based on the human knowledge of system behavior. Matlab/Simulink

p-ISSN: 2348-6848
e-ISSN: 2348-795X
Volume 03 Issue 11
July 2016

simulation model is built to study the dynamic behavior of dc-to-dc converter and performance of proposed controllers. Furthermore, design of fuzzy logic controller can provide desirable both small signal and large signal dynamic performance at same time, which is not possible with linear control technique. Thus, fuzzy logic controller has been potential ability to improve the robustness of dc-to-dc converters. The basic scheme of a fuzzy logic controller is shown in Fig 5 and consists of four principal components such as: a fuzzification interface, which converts input data into suitable linguistic values; a knowledge base, which consists of a data base with the necessary linguistic definitions and the control rule set; a decision-making logic which, simulating a human decision process, infer the fuzzy control action from the knowledge of the control rules and linguistic variable definitions; a de-fuzzification interface which yields non fuzzy control action from an inferred fuzzy control action [10].

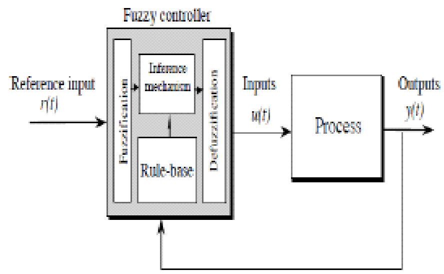

Fig.4. General Structure of the fuzzy logic controller on closed-loop system

The fuzzy control systems are based on expert knowledge that converts the human linguistic concepts into an automatic control strategy without any complicated mathematical model [10]. Simulation is performed in buck converter to verify the proposed fuzzy logic controllers.

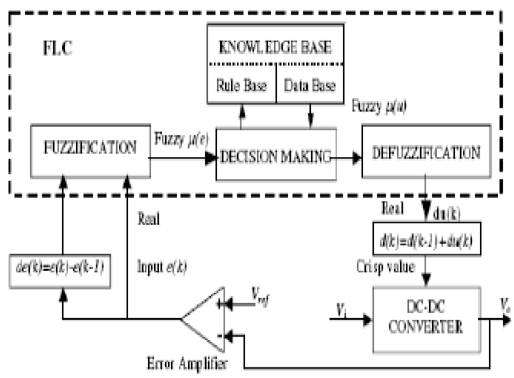

Fig.5. Block diagram of the Fuzzy Logic Controller (FLC) for dc-dc converters

- *Fuzzy Logic Membership Functions:*

The dc-dc converter is a nonlinear function of the duty cycle because of the small signal model and its control method was applied to the control of boost converters. Fuzzy controllers do not require an exact mathematical model. Instead, they are designed based on general knowledge of the plant. Fuzzy controllers are designed to adapt to varying operating points. Fuzzy Logic Controller is designed to control the output of boost dc-dc converter using Mamdani style fuzzy inference system. Two input variables, error (e) and change of error (de) are used in this fuzzy logic system. The single output variable (u) is duty cycle of PWM output.

p-ISSN: 2348-6848
e-ISSN: 2348-795X
Volume 03 Issue 11
July 2016

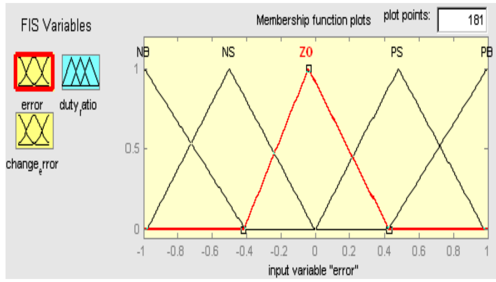

Fig. 6.The Membership Function plots of error

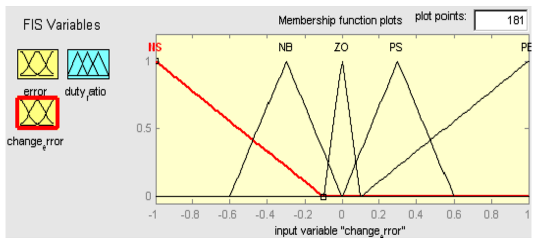

Fig.7. The Membership Function plots of change error

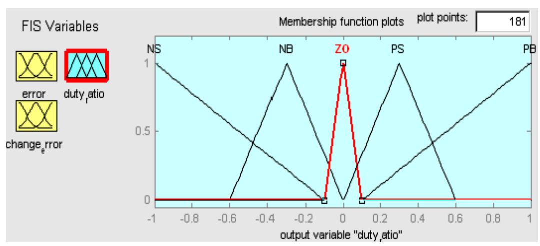

Fig.8. the Membership Function plots of duty ratio

- *Fuzzy Logic Rules:*

The objective of this dissertation is to control the output voltage of the boost converter. The error and change of error of the output voltage will be the inputs of fuzzy logic controller. These 2 inputs are divided into five groups; NB: Negative Big, NS: Negative Small, ZO: Zero Area, PS: Positive small and PB: Positive Big and its parameter [10]. These fuzzy control rules for error and change of error can be referred in the table that is shown in Table II as per below:

Table II
Table rules for error and change of error

(de) \ (e)	NB	NS	ZO	PS	PB
NB	NB	NB	NB	NS	ZO
NS	NB	NB	NS	ZO	PS
ZO	NB	NS	ZO	PS	PB
PS	NS	ZO	PS	PB	PB
PB	ZO	PS	PB	PB	PB

International Journal of Research
Available at https://edupediapublications.org/journals
p-ISSN: 2348-6848
e-ISSN: 2348-795X
Volume 03 Issue 11
July 2016

V SIMULATION RESULTS

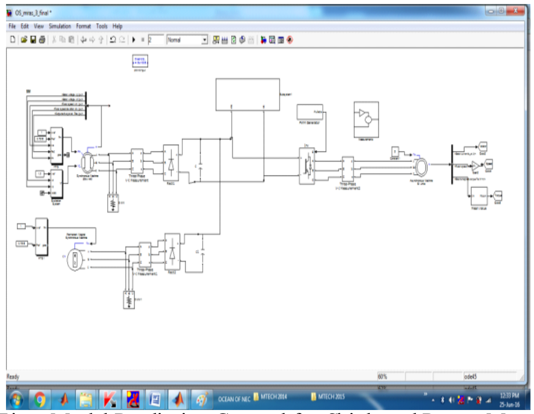

Fig 9 matlab/Simulink circuit of Real-Time Model Predictive Control for Shipboard Power Management Using the IPA-SQP Approach

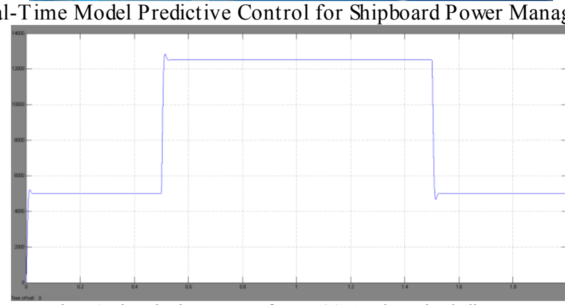

Fig 10 simulation wave form GS-1 Electrical diagram

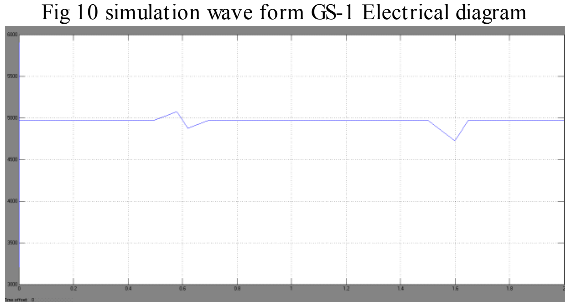

Fig 11 simulation wave form of GS-2 Electrical diagram

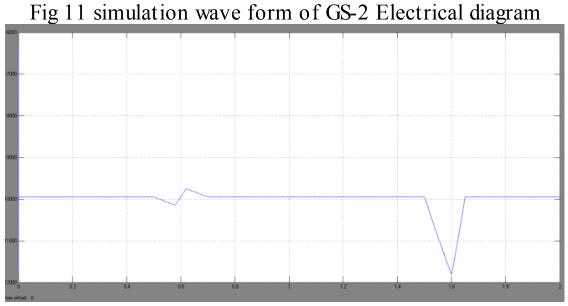

Fig 12simulation wave form of SPS Electrical power

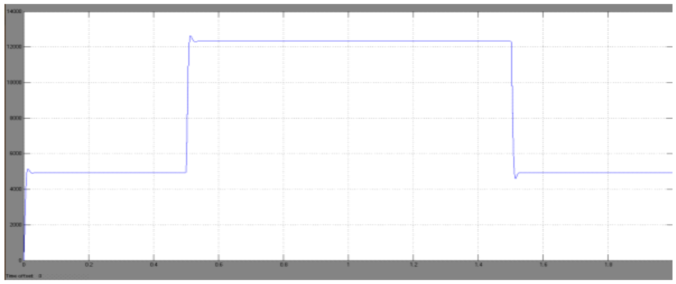

Fig 13 simulation wave form of GS-1 Electrical diagram

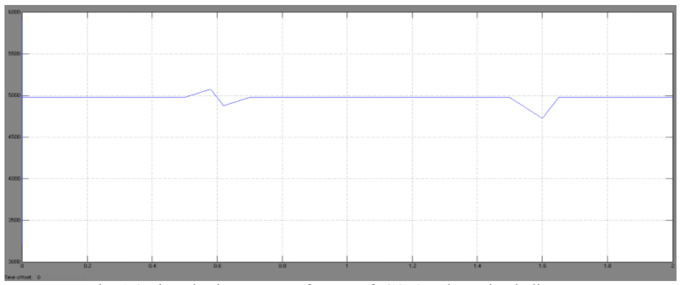

Fig 14 simulation wave form of GS-2 Electrical diagram

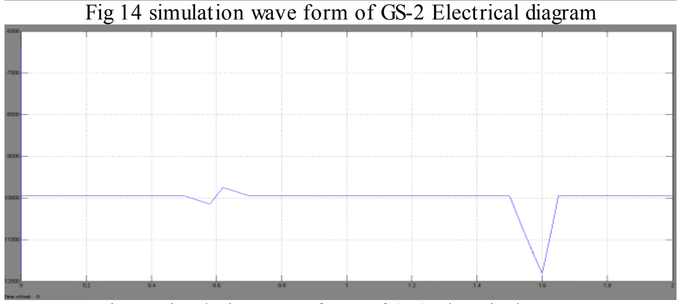

Fig 15 simulation wave form of SPS Electrical power

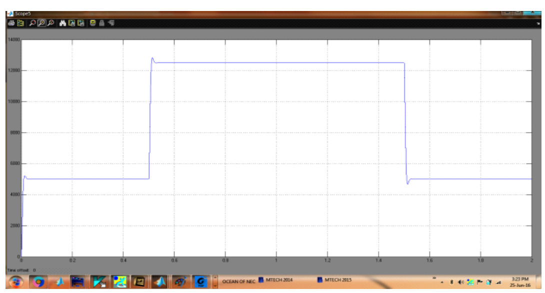

Fig 16simulation wave form voltage and current with fuzzy controller

International Journal of Research
Available at https://edupediapublications.org/journals
p-ISSN: 2348-6848
e-ISSN: 2348-795X
Volume 03 Issue 11
July 2016

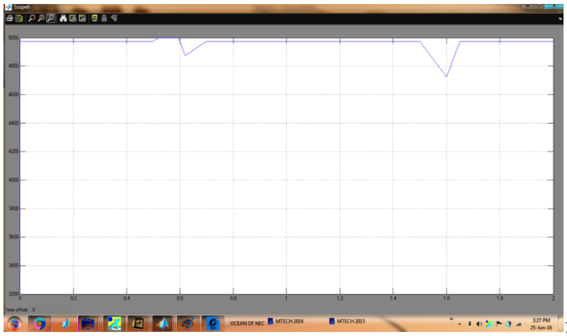
fig 17 simulation wave form of GS-2 Electrical diagram

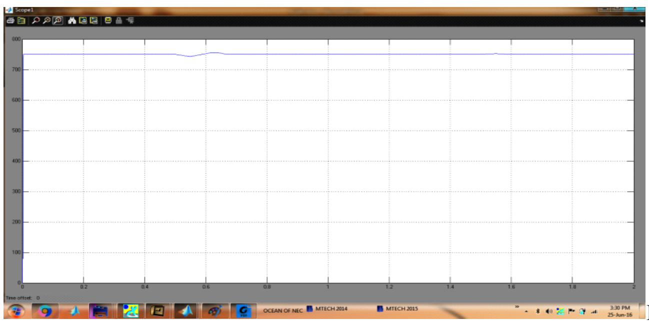
Fig 18 simulation wave form of SQP base output voltage

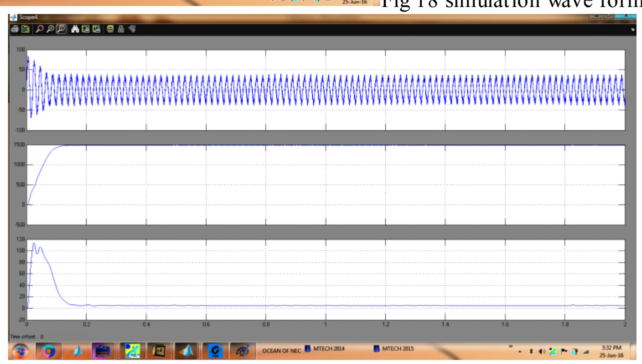

Fig 19 simulation wave form of BLDC drive with stator current, speed and torque with fuzzy logic controller

CONCLUSION

A power management controller for a shipboard power system that uses the IPA-SQP-based MPC has been developed, analyzed, and tested on the simulation model, the Opal-RT real-time simulator, and the physical test bed. The experimental results on the physical test bed and the simulation results are qualitatively correlated. Evaluations of three operational scenarios, Tests A, B, and C, reveal the expected performance sensitivity with respect to tenable parameters, such as the penalties on GS-1 ramp rate and SPS tracking error. The developed PMC successfully allocates requests to power sources and loads in the baseline test with the SWPPL and appropriately modifies control inputs when different aspects of the performance attributes are emphasized by changing weighting factors in the cost function for the MPC problem. This paper demonstrates the feasibility of using the IPA-SQP-based MPC algorithm for real-time power management of shipboard IPS and provides a case that supports further development and implementation of optimization-based PMC for shipboard power systems. TO proposed the fuzzy logic controller and to study the drive characteristic

REFERENCES

[1] N. H. Doerry and J. C. Davis, "Integrated power system for marine applications," *Naval Eng. J.*, vol. 106, no. 3, pp. 77–90, 1994.
[2] N. Doerry and K. McCoy, "Next generation integrated power system: NGIPS technology development roadmap," Naval Sea Syst. Command, Washington, DC, USA, Tech. Rep. 0704-0188, 2007.
[3] G. Seenumani, "Real-time power management of hybrid power systems in all electric ship applications," Ph.D. dissertation, Dept. Mech. Eng., Univ. Michigan, Ann Arbor, MI, USA, 2010.
[4] S. Srivastava and K. L. Butler-Purry, "Expert-system method for automatic reconfiguration for restoration of shipboard power systems,"
IEE Proc.-Generat., Transmiss., Distrib., vol. 153, no. 3, pp. 253–260, 2006.
[5] K. L. Butler-Purry and N. D. R. Sarma, "Self-healing reconfiguration for restoration of naval shipboard power systems," *IEEE Trans. Power Syst.*, vol. 19, no. 2, pp. 754–762, May 2004.
[6] J. M. Solanki and N. N. Schulz, "Using intelligent multi-agent systems for shipboard power systems reconfiguration," in *Proc. 13th Int. Conf. Intell. Syst. Appl. Power Syst.*, 2005, pp. 212–214.
[7] Y. Huang, "Fast reconfiguration algorithm development for shipboard power systems," M.S. thesis, Dept. Elect. Comput. Eng, Mississippi State Univ., Starkville, MS, USA, 2005.
[8] P. Mitra and G. K. Venayagamoorthy, "Real-time implementation of an intelligent algorithm for electric ship power system reconfiguration," in *Proc. IEEE Electr. Ship Technol. Symp.*, Apr. 2009, pp. 219–226.
[9] G. Seenumani, J. Sun, and H. Peng, "Real-time power management of integrated power systems in all electric ships leveraging multi time scale property," *IEEE Trans. Control Syst. Technol.*, vol. 20, no. 1, pp. 232–240, Jan. 2012.
[10] C. E. Garcia, D. M. Prett, and M. Morari, "Model predictive control: Theory and practice—A survey," *Automatica*, vol. 25, no. 3,
pp. 335–348, 1989.
[11] S. J. Qin and T. A. Badgwell, "An overview of nonlinear model predictive control applications," in *Nonlinear Model Predictive Control*. Basel, Switzerland.: Birkhäuser Basel, 2000, pp. 369–392.
[12] S. J. Qin and T. A. Badgwell, "A survey of industrial model predictive control technology," *Control Eng. Pract.*, vol. 11, no. 7, pp. 733–764, 2003.
[13] R. Findeisen and F. Allgöwer, "Computational delay in nonlinear model predictive control," in *Proc. Int. Symp. Adv. Control Chem. Proces.*, 2004, pp. 427–432.
[14] L. Santos, P. Afonso, J. Castro, N. Oliveria, and L. Biegler, "On-line implementation of nonlinear MPC: An experimental case study," *Control Eng. Pract.*, vol. 9, no. 8, pp. 847–857, 2001.
[15] M. Diehl, H. J. Ferreau, and N. Haverbeke, "Efficient numerical methods for nonlinear MPC and moving horizon estimation," in *Nonlinear Model Predictive Control*. Berlin, Germany: Springer-Verlag, 2009, pp. 391–417.
[16] M. Cannon, "Efficient nonlinear model predictive control algorithms," *Annu. Rev. Control*, vol. 28, no. 2, pp. 229–237, 2004.
[17] B. Houska, H. J. Ferreau, and M. Diehl, "An auto-generated realtime iteration algorithm for nonlinear MPC in the microsecond range,"
Automatica, vol. 47, no. 10, pp. 2279–2285, 2011.
[18] M. Vukov, W. Van Loock, B. Houska, H. J. Ferreau, J. Swevers, and M. Diehl, "Experimental validation of nonlinear MPC on an overhead crane using automatic code generation," in *Proc. Amer. Control Conf.*, Jun. 2012, pp. 6264–6269.
[19] M. Diehl *et al.*, "Real-time optimization for large scale processes: Nonlinear model predictive control of a high purity distillation column," in *Online Optimization of Large Scale Systems*. Berlin, Germany: Springer-Verlag, 2001, pp. 363–383.
[20] M. Diehl, H. G. Bock, J. P. Schöder, R. Findeisen, Z. Nagy, and F. Allgöwer, "Real-time optimization and nonlinear model predictive control of processes governed by differential-algebraic equations," *J. Process Control*, vol. 12, no. 4, pp. 577–585, 2002.